doublecortin-like kinase Functions with *doublecortin* to Mediate Fiber Tract Decussation and Neuronal Migration

Hiroyuki Koizumi,[1] Teruyuki Tanaka,[1] and Joseph G. Gleeson[1,*]
[1] Neurogenetics Laboratory
Department of Neurosciences
University of California, San Diego
La Jolla, California 93093

Summary

The potential role of *doublecortin* (*Dcx*), encoding a microtubule-associated protein, in brain development has remained controversial. Humans with mutations show profound alterations in cortical lamination, whereas in mouse, RNAi-mediated knockdown but not germline knockout shows abnormal positioning of cortical neurons. Here, we report that the *doublecortin-like kinase* (*Dclk*) gene functions in a partially redundant pathway with *Dcx* in the formation of axonal projections across the midline and migration of cortical neurons. Dosage-dependent genetic effects were observed in both interhemispheric connectivity and migration of cortically and subcortically derived neurons. Surprisingly, RNAi-mediated knockdown of either gene results in similar migration defects. These results indicate the *Dcx* microtubule-associated protein family is required for proper neuronal migration and axonal wiring.

Introduction

Understanding the molecular basis of cytoskeletal modulation has emerged as an important consideration in developmental neurobiology. The brain is assembled in multiple concurrent steps that rely critically on modulation of the cytoskeleton through a host of control elements. Microtubule-associated proteins are key among these and are important for both initiating and maintaining neurite growth, stabilizing growth cones, and mediating neuronal migration in response to extracellular and intracellular signals.

Regulation of the microtubule cytoskeleton is thought to be important for multiple stages in the developing brain. After mitosis in the proliferative zone, neurons undergo a complex series of morphological alterations in polarity before leaving the subventricular zone (Noctor et al., 2004). As neurons migrate, they repeat of two distinct events that leads to net neuronal displacement: neurite extension followed by nuclear translocation (Gregory et al., 1988; Hatten, 2002). During migration and after reaching cortical target zones, neuronal connectivity is established through axonal and dendritic extension (Auladell et al., 2000). Genetic analysis has highlighted the importance of regulators of the neuronal microtubule cytoskeleton for migration and axonal growth. Mutation in *DCX* (des Portes et al., 1998; Gleeson et al., 1998), *LIS1* (Reiner et al., 1993), *Map1/2* family members (Takei et al., 2000), and *KIF2A* (Homma et al., 2003) among others lead to disordered neuronal migration in a variety of organisms. Similarly, mutations in *tau* (Dawson et al., 2001; Harada et al., 1994), *JNK1* (Chang et al., 2003), or *Map1b* (Del Rio et al., 2004) lead to abnormalities in neuronal morphology, particularly in axonal length and diameter.

Classical lissencephaly is one of the most severe disorders of neuronal migration in humans, but it has been difficult to model this condition in mouse. It is characterized by an agyric cortex with severely impaired lamination, and associated with mutations in two different genes, *DCX* and *LIS1* (reviewed in Kato and Dobyns [2003]). Germline dosage reduction in *Lis1* in mouse was associated with progressive alterations in neuronal targeting to specific laminae within the cortex and hippocampus as gene dosage was reduced (Gambello et al., 2003; Hirotsune et al., 1998). Germline *Dcx* targeting was associated with a hippocampal lamination defect, but cortical lamination was unaffected (Corbo et al., 2002). The lack of a cortical defect in the *Dcx* knockout suggests several fascinating explanations, one of which is genetic redundancy with a *Dcx*-like gene in mouse.

Intriguingly, in rodent, acute RNAi-mediated inactivation of DCX by electroporation of a target plasmid results in both cell-autonomous as well as cell-nonautonomous defects in neuronal targeting to the cortical plate (Bai et al., 2003). As a result, neurons are aberrantly located in the intermediate zone of the brain and display alterations in neuronal morphology. This suggests that DCX in mouse may be required for morphologic changes during neuronal migration. The fact that DCX RNAi shows a phenotype that is not present in the germline gene knockout suggests several other potential explanations that have not yet been explored (reviewed in Gotz [2003]). To our knowledge, this is the first demonstration of a gene that shows a significantly worse phenotype after RNAi versus knockout effects.

The *Dclk* gene (*doublecortin-like kinase*, previously referred to as *KIAA0369* or *Dcamkl1*) encodes a protein with the highest reported homology to DCX across its entire predicted protein sequence, but its function is unknown. It encodes a microtubule-associated protein with a C-terminal serine-threonine kinase domain, although kinase activity is not required for microtubule interactions (Lin et al., 2000; Matsumoto et al., 1999). There are at least three major splice variants: a full length isoform (DCLK), a DCX-domain isoform (DCLK DCX-like), and a kinase domain only isoform (CPG16) with only partially overlapping expression profiles (Burgess and Reiner, 2002; Friocourt et al., 2003). The embryonic forms, DCLK and DCX like, are expressed in populations of migrating neurons that also express DCX (Omori et al., 1998). Furthermore, in cultured neurons, localization to microtubules overlaps with DCX, with the strongest expression in neurite tips (Burgess and Reiner, 2000) and in the vicinity of the cell soma around the nucleus (Lin et al., 2000). This homology and expression pattern supports potential functional redundancy with DCX. In order

*Correspondence: jogleeson@ucsd.edu

to test the role of DCLK in its function with DCX, we targeted DCLK with knockout and RNAi strategies. We found that these strategies produced dosage-dependent effects in neuronal migration and interhemispheric commissure formation.

Results

Targeting Exon 3 of the *Dclk* Gene

The mouse *Dclk* gene is encoded from 20 exons that spans approximately 300,000 bp of genomic DNA on chromosome 3 (Figure 1A). Because of the complex splicing and the fact that the adult isoform, CPG16, (candidate plasticity gene-16, lacking a DCX domain [Nedivi et al., 1993]) utilizes an alternative promoter, we decided to target the 5′ end of the gene. We targeted exon 3 of the *Dclk* gene by a conditional approach (Figure 1B). We did this for several reasons. First, exon 2 is the first coding exon, and removal of exon 3 is predicted to result in splicing of exon 2 to a downstream exon (either 4 or 5) and in both instances will result in out-of-frame splicing. Second, exon 3 encodes the majority of the R1 repeat, a key functional domain (Kim et al., 2003). Third, targeting the N-terminal half of DCLK is predicted to disrupt both full-length DCLK as well as DCLK DCX like. We felt it was important to remove the DCLK DCX-like isoform because this shortened transcript is almost identical to DCX (Friocourt et al., 2003) and would be intact in C-terminal targeting. Finally, to avoid the possibility of embryonic lethality that would preclude examination of brain development, we chose to utilize a conditional targeting approach. We designed a targeting strategy to surround exon 3 with loxP sites. Homologous recombination was detected in 12 clones, and two were injected into blastocysts. High-grade chimeric mice were recovered and mice with germline transmission were subsequently bred to *EIIa-Cre* transgenics (Laksok et al., 1996) in order to mediate germline excision of exon 3. We recovered multiple heterozygous mice, which were subsequently bred to homozygosity. The phenotype of mice from both germline transmissions was not notably different, so only one is discussed here.

Gene Targeting of Exon 3 Removes Isoforms Containing the DCX Domain but Leaves the CPG16 Protein Intact

Expression of each isoform was determined by Western analysis from adult and P1 brain with antisera raised against peptides corresponding to the N- and C-terminal residues (Figure 1C). In wild-type controls, with either antisera, the DCLK isoform was detected at both adult and P1 time points. It was reduced by approximately 50% in the $Dclk^{+/-}$ genotype and was undetectable in the $Dclk^{-/-}$ genotype. We found that the exclusively adult-expressed CPG16 was not altered in either the +/− or −/− genotype. We detected the DCLK DCX-like splice variant as a major band at the predicted molecular weight of 40 kDa in the +/+ mice at P1 but not adult with the N-terminal antibody. This isoform was absent in $Dclk^{-/-}$ littermates at P1. The data suggests that all known isoforms of DCLK containing a DCX-domain are removed with this targeting strategy.

We next tested whether gene targeting resulted in altered compensatory expression of DCX or DCK2. A C-terminal antibody did not detect any DCX at the adult time point and produced a doublet at P1, corresponding to the phospho- and nonphosphospecies. There was no appreciable difference in DCX band intensity in $Dclk^{+/+}$ and −/− brain. Furthermore, there was no appreciable difference in the intensity of the phospho-isoform band, suggesting that DCX is not a direct target of DCLK kinase activity. DCK2 is a separate gene with 70% amino acid similarity to DCLK over the open reading frame that is also expressed in developing brain (Edelman et al., 2004). To test its expression, we created antisera to mouse DCK2 with an N-terminal peptide immunogen. The peptide sequence diverges from DCLK by two amino acids, so it was predicted to react specifically with DCK2 and not DCLK. However, even the affinity-purified antibody detected both DCLK and DCK2 robustly, but because these bands displayed different mobility on Western, it was possible to differentiate them. In both adulthood and P1 the DCLK band was absent in the $Dclk^{-/-}$. Notably, band intensity of DCK2 was indistinguishable in the three DCLK genotypes. We conclude that DCLK deletion does not result in significant compensatory altered expression of DCX, CPG16, or DCK2.

DCLK Expressed in Commissural Axons and Migrating Neurons during Development

To determine the likely sites of action of DCLK during development, we performed immunohistochemistry across developmental time points and compared these with expression of known markers. At E17, expression was strongest in subcortical axonal fiber tracts, especially in the intermediate zone (IZ) just beneath the cortical plate and in the internal capsule (IC), containing cortical efferent and afferent fibers. Expression was compared with L1CAM, an axonal marker that highlights major projections (Chung et al., 1991). We found partially overlapping localization in these fiber tracts (Figures 2A–2C). Prominent expression was noted in fiber tracts that decussate at the midline, most notably the corpus callosal (CC), anterior commissure (AC), and hippocampal commissure (HC) tracts and in the intermediate zone fiber tract. There was little expression in the cortical plate (CP) at this late developmental stage. Identical immunostaining patterns were observed with the N- and C-terminal DCLK antibodies (data not shown). Therefore, at late developmental stages, DCLK is expressed most strongly in axonal fiber tracts.

We next compared expression of DCLK with DCX during development. We found robust and overlapping expression patterns, notably in regions of containing migrating neurons in the CP and in subplate-intermediate zone (SP/IZ) fibers tracts (Figures 2D–2F). DCLK and DCX were coexpressed strongly in commissural axonal tracts of the CC, AC, and HC. Immunostaining of neuronal cultures showed strong overlapping subcellular distribution as well around the cell soma and throughout the growth cone (Figure 2G). The DCLK antibody showed no neuronal signal in $Dclk^{-/-}$ brain sections (data not shown), indicating specificity of the signal. The data suggest that DCLK is codistributed with DCX in migrating neurons and commissural axons during development.

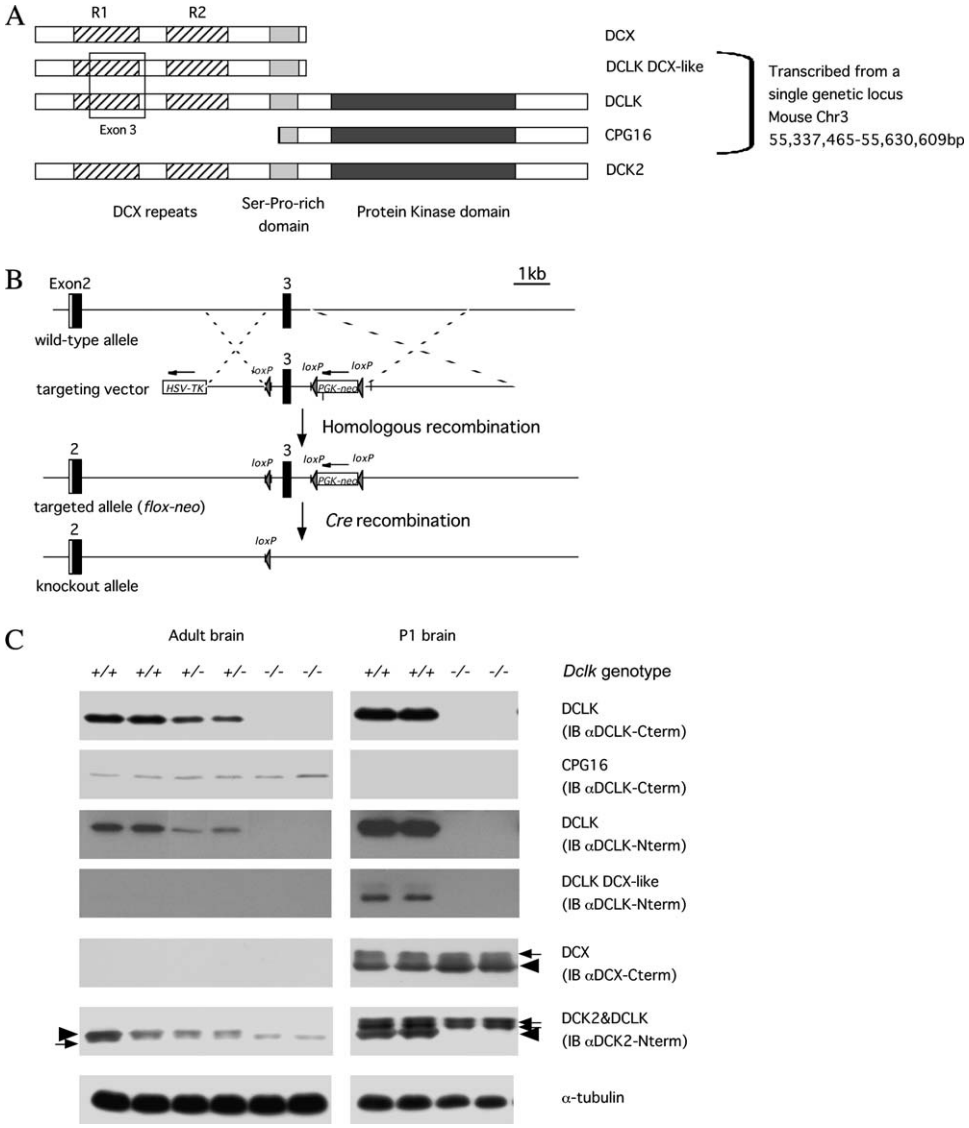

Figure 1. Absence of N-Terminal DCX-Domain-Containing Isoforms after Targeting of *Dclk* Exon 3

(A) The *Dclk* locus encodes for at least three major partially overlapping transcripts, two of which share significant homology with DCX. These transcripts encode DCX-like, containing exclusively the N-terminal half of DCLK, DCLK, containing the DCX-domain and a kinase domain, and CPG16, containing predominantly the kinase domain. The DCX domain contains a duplicated tubulin binding domain (R1 and R2) and a serine-proline-rich domain. An additional gene, DCK2, shares homology with DCLK and is encoded at a different locus.

(B) Targeting strategy for the *Dclk* gene. Exon 3 was targeted by a conditional strategy with HSV-TK as a negative and PGK-neo as a positive selection marker. Homologous recombination led to a conditional targeted allele (flox-neo). Complete removal of exon 3 was mediated by *Cre* recombinase, leading to a germline null allele. In this allele, exon 2 is predicted to splice into exon 4, leading to an out-of-frame null mutation.

(C) Targeting exon 3 of *Dclk* abolishes encoded proteins containing the DCX domain. Adult or postnatal day 1 (P1) brain lysate analyzed by Western blot. Row 1 immunoblotted (IB) with αDCLK-Cterm, showed reduction in +/− and absence in −/− brain. Row 2 IB with αDCLK-Cterm showed expression of CPG16 was not altered in the −/− and was expressed only in adulthood. Row 3 IB with αDCLK-Nterm showed reduction in the +/− and absence in −/− brain. Row 4 IB with αDCLK-Nterm showed expression of DCLK DCX like was exclusively detected in developing brain and was absent in −/− brain. Row 5 IB with αDCX-Cterm showed expression of DCX was not significantly altered (arrowhead). Note that DCX was not hypophosphorylated (normal intensity of upward shifted band, arrow) in the −/−, suggesting DCX is not a direct kinase target of DCLK. Row 6 IB with αDCK2-Nterm showed that this antibody recognized both DCK2 (single arrow at adult, double arrow at P1) as well as DCLK (arrowhead) because the band highlighted by the arrowhead is absent in the −/− lysates. DCK2 level was not altered in −/− brains. Row 7 IB tubulin loading control.

Absence of the Corpus Callosum in the *Dclk*$^{-/-}$ Mutant

We found that *Dclk* homozygous knockout mice were viable and fertile and were recovered at Mendelian ratios in adulthood. The brains were examined for alterations in structure after Cresyl violet staining. We found that there was absence of the CC in *Dclk*$^{-/-}$ mice and presence of Probst bundles (PB) (Figures 3A and 3B). HC was also abnormal (see below). PBs are often identified in mutants with absence of the CC, where they are thought to represent axonal terminals that failed to cross at the midline (Ozaki and Wahlsten, 1993). Notably, the

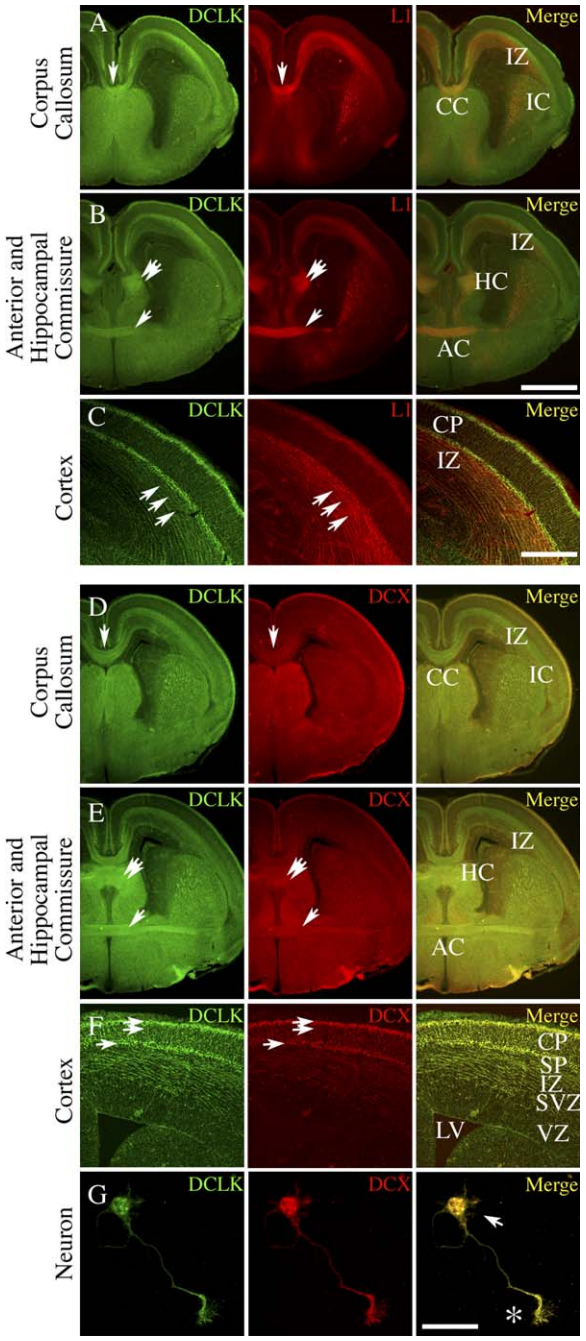

Figure 2. DCLK Codistribution with L1CAM and DCX during Development

(A–B) DCLK codistributed with L1 (a marker of axonal tracts) in the corpus callosum (CC), anterior commissure (AC), and hippocampal commissure (HC) and to a lesser extent in the corticothalamic fibers of the intermediate zone (IZ) and internal capsule fibers (IC). Although DCLK distribution was more widespread than L1CAM, it was enriched in these fiber bundles.

(C) High power showing axonal IZ tracts that colabeled with DCLK and L1 (arrows).

(D–E) Codistribution of DCLK and DCX in the CC, IZ, IC, AC, and HC fiber tracts (arrows).

(F) Coexpression of DCLK and DCX in neurons during periods of migration, especially at the upper (double arrows, corresponding to newly arrived neurons) and lower (arrows) margins of the CP. CP, cortical plate; SP, subplate; SVZ, subventricular zone; VZ, ventricular zone; LV, lateral ventricle.

hippocampus in the −/−, although somewhat misshapened and foreshortened likely as a result of abnormalities of the CC and the HC, displayed lamination indistinguishable from wild-type (wt), and the AC was well formed.

We determined if the absence of the CC phenotype was subject to variable severity or expressivity in the *Dclk* mice because defects can occur spontaneously in some strains (Ozaki and Wahlsten, 1993). Therefore, we sectioned through the A/P dimension of the CC in brains from five mice of each +/+, +/−, and −/− genotypes and examined serial sections. We found that the +/+ littermates in the mixed background displayed uniform appearance of the CC along the rostro-caudal axis. In contrast, homozygous mutant mice displayed uniform abnormalities of the CC along the entire A/P dimension. The appearance of the PB, although uniformly present, was variable in dimension. Surprisingly the +/− mice displayed occasional alterations in CC thickness, with the appearance of small PB, suggesting dosage-dependent effects of DCLK. However, the CC was found to be at least partially intact in each of the +/− mice examined. We conclude that DCLK plays a critical role in CC development.

Intact cortical Lamination in the *Dclk*$^{-/-}$ Mouse

The strong expression of DCLK in populations of neurons in regions of migration prompted us to test for a defect in neuronal migration that might underlie the CC agenesis. Cresyl violet staining of the cortical plate at the P0 and adult time points revealed no alteration in histological appearance (Figure 3A and data not shown). To test for defects in lamination, we performed BrdU birthdating of the cortical neurons by dam injection at E15.5 and E12.5 to label newly dividing cells that will populate layers 2/3 and 5/6, respectively (Gambello et al., 2003). These time points were chosen because layer 2/3 neurons presumably traverse the greatest distance and thus should be among the most sensitive to genetic alterations. Additionally, layers 2/3 make major contributions to the CC (Hedin-Pereira et al., 1999), whereas layer 5/6 neurons are among the earliest to arrive at the cortical plate. BrdU at these time points strongly labeled the appropriate layers, with some scattered positive cells throughout the rest of the cortical wall. We found no discernable difference between +/+ and −/− brains. This effect was quantitated by bin analysis, by dividing the cortical wall into ten equally spaced divisions, and determining the percentage of neurons in each bin. No defect in birthdating was apparent (Figures 3C–3F). The data suggest that the *Dclk*$^{-/-}$ mice do not display significant alterations in cortical neuronal lamination or migration.

Interhemispheric Projection Selectively Disrupted in the *Dclk*$^{-/-}$ Mouse

We sought to determine if there was a general failure of axonal projections or a selective disruption in interhemispheric CC axonal projections. To differentiate between

(G) Cultured cortical neuron showing subcellular codistribution of DCLK and DCX in the cell soma (arrow) and growth cone (asterisk). N-terminal polyclonal antibody was used for all the DCLK staining. (A)–(E) are E17 and (F) and (G) are E15. Size bar: low power, 1.5 mm; high power, 0.5 mm; G, 20 μM.

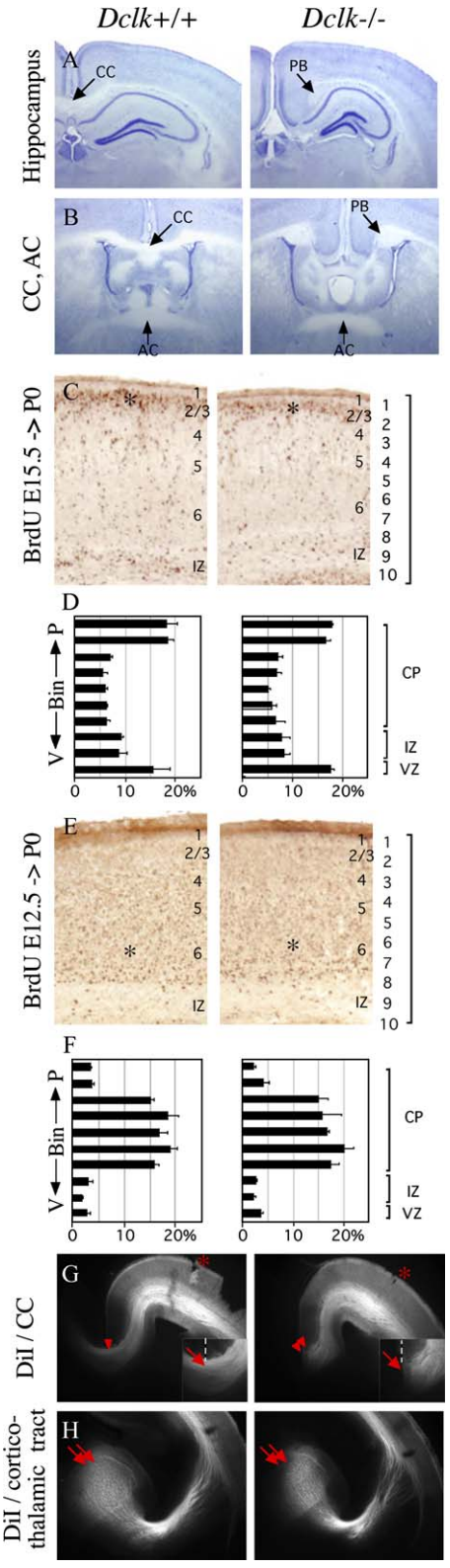

Figure 3. *Dclk*$^{-/-}$ Is Associated with Absence of the Corpus Callosum but Intact Anterior Commissure and Cortical Lamination

(A and B) Adult brain stained with Cresyl violet showed indistinguishable hippocampal and cortical lamination but absence of the corpus callosum (CC) in *Dclk*$^{-/-}$. In place of the CC, Probst bundles (PB) were evident, indicating failed axonal decussation. The anterior commissure (AC) is intact.

these possibilities, we performed DiI injections into the lateral cortex at E17.5 to label efferent and afferent axonal tracts. In wt brains we detected DiI signal in the corticothalamic (CT) as well as the CC pathway where it crossed the midline. In *Dclk*$^{-/-}$ brains, the CT projection was of normal appearance, but the interhemispheric CC axons failed decussate (Figures 3G and 3H). Higher power views indicated that axons failed to extend across the midline. The results suggest a selective requirement for *Dclk* specifically in the axonal projection of the CC.

Dosage-Dependent Interactions between *Dclk* and *Dcx* in Commissural Fiber Tract Formation

The striking sequence similarity and overlapping expression profile of *Dclk* and *Dcx* suggested potential functional redundancy in neuronal development. To determine if there were genetic interactions between *Dclk* and *Dcx* in adulthood, we bred heterozygous *Dclk* and *Dcx* mice and then intercrossed to obtain double knockout mice. Genotyping of the pups from these matings showed that double knockout mice (*Dclk*$^{-/-}$*;Dcx*$^{-/y}$ or *Dclk*$^{-/-}$*;Dcx*$^{-/-}$) died before weaning, consistently right after the time of birth, suggesting functional redundancy.

We initially focused our attention on the interhemispheric connections because this was the major site of defect in the *Dclk*$^{-/-}$ mouse. Horizontal sections were obtained through the three major interhemispheric tracts, the CC, HC, and AC and stained for L1, a marker for these tracts. We found that deletion of *Dcx* alone had no effect on the morphology of the CC, HC, or AC at P0 (Figure 4). In the *Dclk*$^{-/-}$ mutant, we noted absence of the CC, as well as absence of the HC, whereas the AC appeared of normal morphology and thickness. In the *Dcx*-null genetic background, as dosage of *Dclk* was reduced from +/+ to +/−, we noted that the CC was hypoplastic and the AC was severely reduced in thickness, whereas the HC was normal in appearance. Similarly, in the *Dclk*$^{-/-}$ genetic background, as dosage of *Dcx* was reduced from +/+ to +/−, we noted that the AC was hypoplastic. Removal of all four gene copies resulted in absence of the CC, HC, and AC. PBs were apparent in each of the mice with absence or hypoplasia of the CC. We conclude that *Dclk* plays a major role in determining the development of the CC and HC, whereas *Dclk* and *Dcx* cooperate to mediate formation of the AC during development. The data suggests that there are significant genetic interactions between *Dclk* and *Dcx* during development.

(C–F) BrdU injection at E15.5 or 12.5 examined at P0 showed indistinguishable cortical lamination birthdating patterns in +/+ and −/−, labeling predominantly layer 2/3 (asterisk) or 5/6 (asterisk), respectively, though scattered positive neurons were identified in other layers. (D and F) The cortical wall was divided into ten equal bins from ventricle (V) to pial (P) surface. No discernable differences were apparent. n > 1200 cells per genotype from three serial sections. Error bar, SEM.

(G and H) DiI injection at E17.5 (site indicated by an asterisk) showed intact corticothalamic projections (double arrows in [H]) but failure of CC projections (double arrowheads indicate PB in [G]). Inserts show higher-power crossing (arrow) at midline (dashed) in +/+ but failure in −/−. Representative images from at least three mice of each genotype.

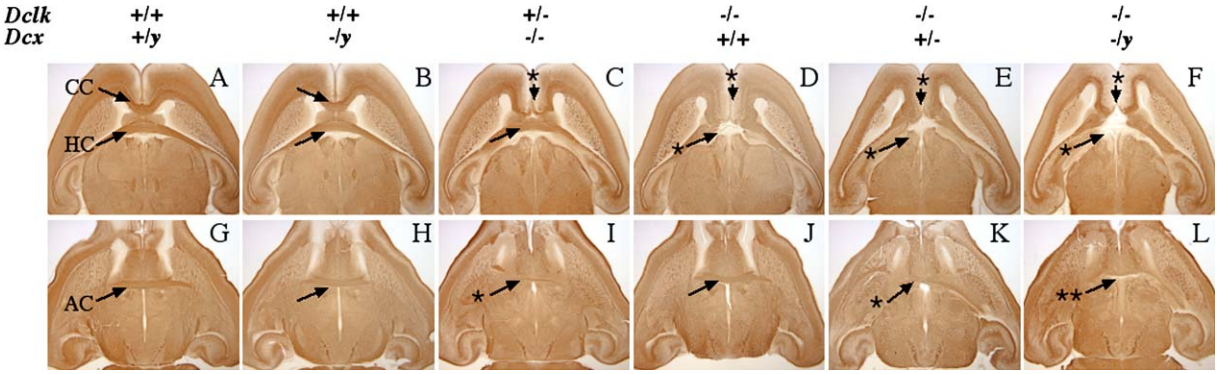

Figure 4. Dosage-Dependent Effects of DCLK and DCX on Commissural Axonal Formation

(A, B, G, and H) No discernable defect in interhemispheric connections in the *Dcx*$^{-/y}$ mutant.

(C and I) Removal of one *Dclk* allele from the *Dcx*-null background led to absence of the CC (asterisk) and hypoplasia of the AC (asterisk).

(D and J) The *Dclk*$^{-/-}$ mutant shows absence of the CC (asterisk) and HC (asterisk) but normal appearance of the AC.

(E and K) Removal of one *Dcx* allele from the *Dclk*$^{-/-}$ background led to hypoplasia of the AC (asterisk) in addition to absence of the CC (asterisk) and HC (asterisk).

(F and L) Removal of all four alleles led to absence of CC (asterisk), AC (asterisk), as well as HC (double asterisk). Representative images from at least three mice of each genotype.

Dosage-Dependent Defects in Cortical Cytoarchitectonics

Given the strong codistribution of proteins in migrating neurons during development and lack of evidence that the single mutations in mice are associated with a neuronal migration defect, we tested whether inactivation of both *Dclk* and *Dcx* was associated with disordered cortical lamination. Sections from *Dclk*$^{+/+}$;*Dcx*$^{+/y}$ and *Dclk*$^{-/-}$;*Dcx*$^{-/y}$ mice were stained with Tst-1, a marker of layer 2/3 and 5 neurons (Frantz et al., 1994). We found a striking cortical lamination defect, which was most notable in lateral cortex, and gradually lessened in ventral and dorsal regions (Figure S1). We conclude that *Dclk* and *Dcx* cooperate to mediate cortical lamination in mice.

In order to determine the relative contributions of each gene on neuronal migration, we studied an allelic series of double knockout mice with Cresyl violet. Because of the regional differences in severity seen in the double knockout, we carefully chose anterior-posterior-matched sections and imaged in the same relative lateral region of cortex. Cresyl violet staining revealed a dosage-dependent effect on cortical lamination that was apparent as alleles were removed in a stepwise fashion. Wt mice showed the typical lamination pattern of a cell-poor marginal zone, a cell-rich layer 2/3 and 5, with relatively less cell-dense layers 4 and 6 (Figure 5A). Removal of one copy of *Dclk* in the *Dcx* mutant background (i.e., *Dclk*$^{+/-}$;*Dcx*$^{-/y}$) showed disrupted cytoarchitectonics, with a dispersion of the cell-rich layer 2/3 region. Removal of one copy of *Dcx* in the *Dclk* mutant background (i.e., *Dclk*$^{-/-}$;*Dcx*$^{+/-}$) showed similar disrupted cytoarchitectonics based on Cresyl violet staining, although it appeared somewhat more severe than the *Dclk*$^{+/-}$;*Dcx*$^{-/y}$. The interpretation of this experiment is complicated by the fact that *Dcx*$^{+/-}$ female mice are mosaics for the *Dcx*$^{+}$ and *Dcx*$^{-}$ allele, and the percentage of cells expressing null versus wild-type DCX is dependent on X-inactivation patterns. However, this finding was not simply due to rare skewed X-inactivation patterns, because it was noted in all tested females of the genotype *Dclk*$^{-/-}$;*Dcx*$^{+/-}$ (n = 3). Finally, removal of all four alleles resulted in completely disrupted cytoarchitectonics, without apparent laminar structure to the cortex.

Double Knockout Mice Display Severe Disruption of Cortical Neuronal Migration

In order to test for a defect in migration, we performed immunohistochemical analysis with E15.5 injection of BrdU and lamina-specific markers with the same four genotypes. Analysis of BrdU staining at P0 in wt resulted in a somewhat broadened distribution of positive cells, but the grouping of approximately 10% of neurons at the top of the cortical plate (layer 2/3) was evident (Figures 5B and 5C). (Because litters containing double knockouts are consistently born 1/2–1 day earlier (at E18–18.5) than litters containing only single knockouts (at E19–19.5), the BrdU results in wt were not as distinct compared with Figure 3C.) We noted a shift in the bin distribution of labeled neurons toward deeper cortical layers in each of the mutant genotypes. In *Dclk*$^{+/-}$;*Dcx*$^{-/y}$ and *Dclk*$^{-/-}$;*Dcx*$^{+/-}$ mutant mice, there were fewer BrdU-positive neurons in this region, comprising approximately 5%–7% of total BrdU-positive cells. In the *Dclk*$^{-/-}$;*Dcx*$^{-/-}$, even fewer were apparent at the top of the cortical plate, comprising approximately 3% of total BrdU-positive cells. There was no more than a 10% difference in the total number of labeled cells among the four genotypes (data not shown). The data suggests that dosage reduction in the *Dclk*/*Dcx* genes results in cortical neuronal migration defects.

Marker analysis was performed with Tst-1 and Tbr-1, which at P0 labels cortically derived neurons destined for layer 2/3 and 5 (Frantz et al., 1994), and layer 6 and subplate (Hevner et al., 2001), respectively. We found a striking alteration in the normal distribution of these neurons compared with wt. Tst-1 staining in the mutants showed a broad pattern of distribution, with labeled neurons extending across a much wider distance at the top of the cortical plate (Figure 5D). The degree of abnormality was more severe as gene dosage was reduced. Tbr-1 staining also showed a broader distribution, with positive neurons positioned in more superficial

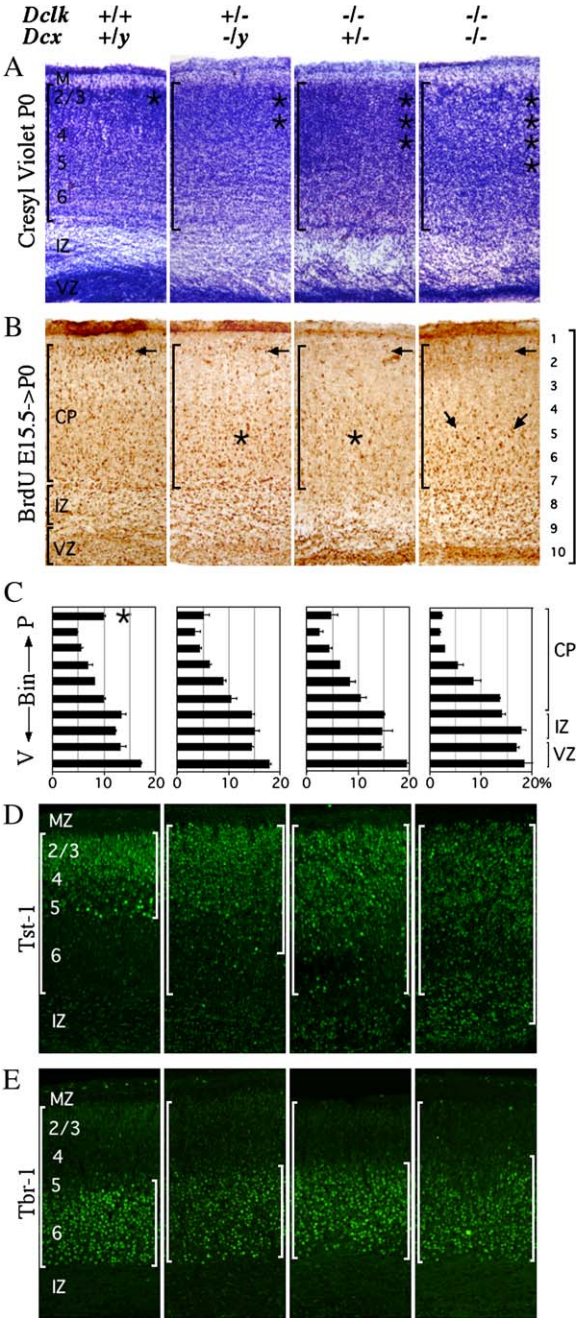

Figure 5. *Dclk* and *Dcx* Cooperate to Mediate Cortical Neuronal Migration

(A) Cresyl violet staining shows normal cortical plate (CP) width (bracket) and location of the intermediate (IZ) and ventricular zone (VZ) in $Dclk^{+/+};Dcx^{+/y}$. Note high density of cells in the upper cortical plate in layer 2/3 (asterisk). The latter three genotypes ($Dclk^{+/-};Dcx^{-/y}$, $Dclk^{-/-};Dcx^{+/-}$, and $Dclk^{-/-};Dcx^{-/-}$) showed progressive dispersion of cells within the CP toward deeper layers (asterisk shows extent of cell dispersal).

(B) BrdU injected at E15.5 analyzed at P0 showed a collection of positive cells in layer 2/3 in wild-type (arrow), with progressively fewer positive cells in upper layers (arrows) and more in deeper cortical layers (asterisk) as gene dosage was reduced. In $Dclk^{-/-};Dcx^{-/-}$ the majority of positive neurons within the CP were at the bottom (arrows).

(C) Bin distribution of BrdU-positive cells (E15.5 injection → P0 analysis). The collection of neurons present in bin 1 (asterisk) was diminished as gene dosage was reduced. n > 2000 cells per genotype from three serial sections. Error bar, SEM.

(D) Tst-1-positive cells were mainly present in layer 2–3 of the CP (left brackets) at P0 in wt but showed a progressively broadened distribution (right brackets) in the latter three genotypes. The majority of neurons were evident in the upper parts of the cortex in the middle two genotypes, indicating that the CP was not inverted. In the $Dclk^{-/-};Dcx^{-/-}$ the cells were apparently evenly distributed across the cortex.

(E) Tbr-1 staining showed predominantly layer 5/6 staining at P0 in wt but a progressively broadened distribution in the latter three genotypes. Representative images from at least three mice of each genotype.

regions of the cortex compared with wt (Figure 5E). These results suggest both a broadening of the normal laminae as well as a scattering of positive neurons in other cortical regions. We compared these results with those obtained after the same staining in single knockout mice $Dcx^{-/y}$ and $Dclk^{-/-}$, both of which appeared normal (data not shown). The results suggest that *Dcx* and *Dclk* cooperate to mediate positioning of cortical neurons within the correct lamina.

RNAi Targeting of *Dclk* or *Dcx* Result in Similar Neuronal Migration Defects

We were intrigued by the finding that RNAi-mediated knockdown of DCX led to a robust neuronal migration defect in mouse, a finding that was not observed in the *Dcx* germline mutation. We considered that the same result might be found in the case of DCLK, especially because $Dclk^{-/-}$ mice, like the $Dcx^{-/y}$ mice, displayed no cortical lamination defect. To test this, we cloned six different RNAi constructs targeted to mouse *Dclk* in various regions predicted to work well for knockdown, having no other complete matches in the database and not more than a minimal match with any member of the DCX family of genes. These RNAi constructs targeted exon 2, which is invariantly present in isoforms containing the DCX domain. Each construct was tested for its ability to knockdown the DCLK message specifically, without an effect on DCX. We chose two constructs that produced the most robust knockdown effect, based on qualitative immunofluorescence intensity of side-by-side transfected versus nontransfected neurons (Figure S2). Each construct or a negative control was electroporated into the right lateral ventricle of wild-type mice at E13 and examined at E17. Results were performed in at least three mice for each construct and repeated in three separate litters. In parallel experiments, we compared results with those obtained with the construct previously used to target DCX (Bai et al., 2003) (in which the targeting plasmid is electroporated together with a GFP reporter plasmid), with a construct with the same target sequence but cloned into a vector that also encodes GFP (to avoid possible single transfected cells) and with constructs containing two different DCX target sequences. These additional experiments were performed to increase the certainty of specificity of the RNAi knockdown effect. In parallel experiments, we confirmed that none of these DCX siRNA constructs had effect on DCLK expression in cultured neurons (Figure S2).

Electroporation of a negative control GFP siRNA plasmid showed many of the cells positioned in the upper part of the developing cortical plate (Figure 6). In mice electroporated with the DCX sh3′UTR construct (Bai

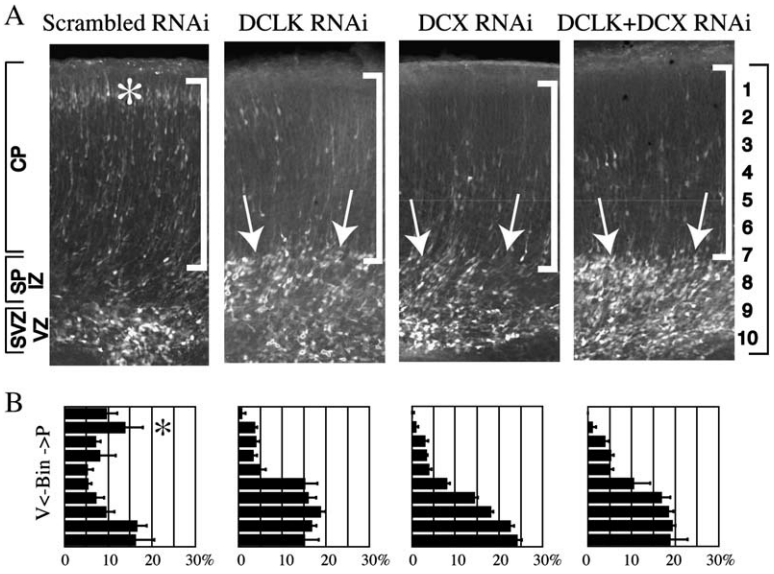

Figure 6. RNAi-Mediated Knockdown of DCLK or DCX Results in Neuronal Migration Defect In Vivo

(A) Electroporation of RNAi constructs to target endogenous DCLK and DCX (also encoding GFP) were electroporated into the right lateral ventricular wall at E13.5 and analyzed at E17.5. In control, positive cells were scattered throughout the width of the cortical mantle, with an appreciable number of cells (asterisk) visible within the upper part of the cortical plate (delineated by white bracket). DCLK or DCX RNAi resulted in few neurons positioned in the upper cortical plate. Instead, most neurons were positioned in deeper regions of the cortical mantle in the subplate (SP) and subventricular (SVZ) zones (arrows). Results repeated in triplicate, and data from one of two DCLK constructs are representative.

(B) Bin distribution of migration distance. The cortical mantle was divided into ten equally spaced bins, and percentage of cells in each bin was represented. In control, approximately 25% of cells were positioned in the upper two bins, whereas RNAi targeting separately or together resulted in few than 10% in upper bins (asterisk). No appreciable difference was noted with single (DCX or DCLK) or double (DCX plus DCLK) RNAi. Data summarizes three serial sections for each condition. n > 250 cells for each condition. Error bar, SEM.

et al., 2003) together with a GFP reporter plasmid, we found that the majority of electroporated neurons were positioned within the subplate, with other positive neurons scattered in other cerebral wall locations as reported (data not shown). Electroporation of a DCX RNAi construct in which the GFP was expressed from the same plasmid produced similar results, with very few labeled cells positioned within the cortical plate. Electroporation of two different DCLK siRNA plasmids produced results very similar to the DCX targeting construct, with cells positioned predominantly in the subventricular and subplate zones. This effect was quantitated by bin analysis, by dividing the cortical wall into ten equally spaced divisions, and identifying the percentage of neurons in each bin. We noted that DCLK or DCX RNAi led to near absence of positive neurons within the upper cortical layers, as was found in the scrambled control, and bin distribution was similar for the DCLK and DCX RNAi experiments. We also compared the effect of double electroporation of constructs to target DCLK and DCX together. In this experiment, we observed few cells in the cortical plate, with most positive cells positioned within the subventricular and subplate zones, comparable to what was observed with either single RNAi construct alone. Bin distribution analysis showed similar results for the single versus double electroporations. We conclude that acute RNAi-mediated knockdown of DCLK results in cortical neuronal migration defects similar to DCX.

Discussion

Here, we show that DCLK is expressed both in populations of neurons during periods of migration, as well as in major cortical axonal fiber tracts during development in a pattern that overlaps with DCX. Homozygous deletion of *Dclk* alone does not produce a hippocampal lamination defect as was observed in the *Dcx* knockout. Instead, *Dclk* is required for formation of the corpus callosum, one of the major interhemispheric axonal fiber tracts. *Dclk* and *Dcx* show redundancy and dosage-dependent genetic interactions in interhemispheric connectivity because stepwise reduction in dose shows progression of phenotype from hypoplasia to aplasia of the CC, HC, and AC and defects in cortical lamination and neuronal migration. Surprisingly, RNAi-mediated gene knockdown of *Dclk* showed an essential function in neuronal migration similar to *Dcx.* Together, the data suggest that *Dclk* and *Dcx* cooperate in axonal tract development and neuronal migration.

Requirement for DCLK in Interhemispheric Connectivity

Our targeting strategy was aimed at determining the role of the DCX domain of the *Dclk* locus. We removed the second coding exon of DCLK that encodes an essential domain, predicted to result in premature protein truncation. We show that this strategy, as predicted, results in absence of both full-length DCLK as well as DCLK DCX like, thus completely removing any DCX-like function from encoded proteins. Additionally, there was no noted compensatory increase in expression of the two other close family members DCX or DCK2.

The primary defect identified in the *Dclk* null mice was agenesis of the corpus callosum. Corpus callosum agenesis is associated with several mouse mutants of diverse genes and human neurological syndromes and consists of fascicles of axons from neurons positioned in predominantly in layer 2/3, but all cortical layers show evidence of projections to the callosum (Yorke

and Caviness, 1975). During development as these neurons are in the intermediate zone en route to the cortical plate, they extend an axon that begins to project toward the midline. The callosal axon remains associated with the radial glia on which the neuron is migrating (Norris and Kalil, 1991). Callosal axons extend through a corridor defined by two midline cell populations, the glial wedge and the indusium griseum (Shu and Richards, 2001), which release chemoactive factors essential for axonal crossing (Shu et al., 2003). Callosal axons decussate across the midline around E16 and do not reach their target until around P2 to P3 (Rash and Richards, 2001).

We considered each of these developmental steps in determining the mechanism of the callosal defect in the *Dclk* mutant. We found no defect in neuronal migration in the $Dclk^{-/-}$ mutant that would account for callosal defect. There was no defect observed in the radial glial scaffold during late prenatal development upon immunostaining for vimentin (Figure S3) or in the structure of the glial wedge or indusium griseum at P0 based on GFAP staining (Figure S4). Finally, we found no defect in projection of intrahemispheric corticothalamic projections upon labeling with DiI. Together, the data suggest a selective requirement for *Dclk* in interhemispheric callosal projections.

This conclusion was further supported by our observation of the interaction of *Dclk* and *Dcx* in the decussation of the AC and HC, the other major long distance interhemispheric commissures. It is possible that these defects are a result of impaired cortical neuronal migration and as a result impaired axonal initiation in the double knockout. However, in all of the genotypes tested, the ipsilateral fasiculus was evident but the commissure failed to cross at the midline following dosage reduction, suggesting a defect in axon elongation or guidance but not initiation.

Genetic Interactions of *Dclk* and *Dcx* in Neuronal Migration

Interactions between *Dclk* and *Dcx* were identified in migration of neurons to the cerebral cortex. Related defects were observed after in utero electroporation, which likely preferentially labels cortically derived neurons rather than interneurons. This leaves open the question whether the migration of interneurons that derive from subcortical locations is also disrupted. Our preliminary data indicates that at least a fraction of these interneurons also fail to migrate correctly because calretinin-positive neurons were not apparent in upper cortical layers in the $Dclk^{-/-}$;$Dcx^{-/-}$ mutant (Figure S5) (Gonchar and Burkhalter, 1997; Kawaguchi and Kubota, 1997). This data suggests the DCX family of genes is implicated in migration of both cortically and subcortically derived neurons. Because subcortically derived neurons are the main source of the inhibitory neurotransmitter GABA in the brain (Lavdas et al., 1999; Xu et al., 2004), this may account for the extremely high incidence of epilepsy observed among patients with *DCX* mutations. Because detailed neuropathological examination in human patients with classical lissencephaly is lacking, it is not possible to compare directly, but we would expect defects in both of these populations.

We noted the neuronal migration defect for cortically derived neurons was most apparent in the upper cortical layers. This may reflect the fact that upper cortical layer neurons have greater migration distances or may reflect other genetic or environmental susceptibilities. We also noted that cytoarchitechtonic defects for both cortically and subcortically derived neurons were most apparent in lateral cortex. The basis for these regional selectivities was not apparent in this study, but similar findings have been reported in humans with *Dcx* mutations, which produce more severe migration abnormalities in frontal as compared with occipital brain regions (Dobyns et al., 1999). Marker analysis excluded an inversion in lamination of the cortical plate, as observed in *reeler*-pathway mutants (Caviness, 1982), and no defect in radial glial morphology was detected in any of the genotypes (Figure S3), supporting a direct role for these genes in migration of neurons.

Given the human double cortex phenotype in $DCX^{+/-}$ women, we tested for this in mice with dosage reduction of *Dclk*, namely in mice with $Dclk^{+/-}$;$Dcx^{+/-}$ and $Dclk^{-/-}$;$Dcx^{+/-}$ genotype. In neither did we observe a heterotopic band of neurons in the subcortical white matter. In contrast, RNAi-mediated knockdown of *Dcx* in rat but not in mouse has shown this effect. Thus, it may not be possible to model this phenotype in mouse with genetic alteration of the *Dcx* pathway, possibly because of the smaller width of the cortical wall. Alternatively, there may be further genetic redundancy with the *Dck2* gene (Edelman et al., 2004).

RNAi-Mediated Knockdown of *Dclk* Shows Migration Defects

We found that RNAi against DCLK alone produced a migration defect in electroporated neurons that was very similar to that observed with DCX RNAi. Neurons were heterotopically located within the subcortical white matter in the vicinity of the intermediate and subplate zone. Surprisingly, RNAi targeting of both DCLK and DCX led to no worsening of the observed migration defect over single RNAi targeting, despite dosage-dependent effects after germline gene inactivation. Although these results appear at odds, it is possible that the phenotype observed after RNAi was terminal and not susceptible to further worsening or that the RNAi machinery was in limiting concentration.

Why does RNAi to DCLK and DCX produce a defect in neuron migration when germline deletion of the gene does not produce this effect? There are several possibilities (Bai et al., 2003; Gotz, 2003) including the following. (1) Acute inactivation via RNAi may not be capable of inducing compensatory mechanisms that are invoked after germline inactivation. (2) Inactivation via electroporation in a subset of cells may lead local disruption of migration. In other words, migration of a mutant cell surrounded by wild-type cells may be more severely affected than a mutant cell surrounded by other mutant cells. (3) RNAi may mediate off-target effects on other neuronal migration genes. We found that RNAi targeting of DCX does not significantly effect DCLK levels and vice versa, and these effects on migration are present with at least two different nonoverlapping RNAi constructs (data not shown), making the last possibility less likely. The first and second possibility can be addressed by testing whether acute gene inactivation with a different method can recapitulate this phenotype,

an experiment that is possible with a conditional allele of *Dclk* that was produced in the course of this study, followed by electroporation of Cre-GFP in embryos. The third possibility can be addressed through demonstration of rescue of the migration defect by coelectroporation with a wild-type gene not susceptible to targeting or by demonstration of no phenotype after electroporation of RNAi into the corresponding knockout. It will be important to address these possibilities in order to fully understand the role of DCX family members in migration.

Selective Requirement for Microtubule Regulators in the Combined Axonal Extension/Neuronal Migration Phenotype

What may be the basis for the genetic interactions between DCX and DCLK? We favor the model in which the molecules function in parallel to mediate microtubule stability during neuronal morphogenesis. Neurite outgrowth is likely required for both neuronal migration and axonal extension, as exemplified by combined phenotype associated with several gene mutations including KAL-1, Ephrins, and Cdk5 (Ohshima et al., 1996; Teng et al., 2001; Zhou et al., 2001). We found no direct effect of RNAi to DCX and DCLK on neurite outgrowth in cultured neurons, however (data not shown). More direct interactions between DCX and DCLK are possible as well. For instance, we found that DCX and DCLK are part of a complex in both transfected cells and in developing brain (Figure S6), suggesting that these may form a heterodimer similar to the homodimer that Dcx has been reported to form (Caspi et al., 2000). Therefore, additional studies may indicate further biochemical modulation of this interaction or its effect on microtubule stability. Together, these studies suggest abundant functional redundancy in modulation of the microtubule cytoskeleton during development.

Experimental Procedures

Gene Targeting

The pflox vector was engineered to translocate the HSV-TK cassette from a site adjacent to the PGK-neo to a site outside of the short arm. PCR amplicons for the short arm, long arm, and exon 3 were created based on the most recent consensus mouse sequence from the C57BL/6 strain (http://www.genome.ucsc.edu/) and used to amplify from 129/SvJ strain. The pflox vector was engineered to introduce HSV-TK gene with PyF (viral polyoma) enhancer, derived from TK1-TK2A vector (kindly gift from Mario Capecchi) (Li et al., 1998) outside of the 3-loxP cassette (kindly gift from J. Marth). Mice carrying the 3-loxP *Dclk* conditional allele were crossed with *EIIa-Cre* transgenic mice (kindly gift from A. Wynshaw-Boris) (Laksok et al., 1996) in order to delete the loxP site. Offspring from these intercross generated *Dclk* heterozygous mice (complete deletion of 3-loxP site) or *Dclk* mosaic mice. *Dclk* heterozygous mice were used for subsequent analysis.

Animal Breeding

Mice were maintained on a mixed background consisting of predominantly 129/SvJ and C57BL/6, *EIIa-Cre* on a mixed 129/SvJ/Black Swiss background, and *Dcx* knockout on a mixed 129/SvJ/Black Swiss background. All experiments were performed on littermates whenever possible and in accordance with UCSD Animal Care Program approved protocols.

Western Analysis

Protein lysates were analyzed on 12% PAGE-SDS gels as described (Tanaka et al., 2004). Antibody to DCLK was made in rabbit against the N-terminal 12 amino acids by standard protocols. Primary antibodies were used at following concentrations: anti-DCLK N-terminal polyclonal antisera, 1;2000; anti-DCLK C-terminal polyclonal antisera, 1:5000; goat polyclonal anti-DCX (sc-8066, Santa Cruz Biotechnology), 1:1000; anti-DCK2 N-terminal polyclonal antisera, 1:2000.

DiI Labeling

E17.5 brains were fixed with 4% paraformaldehyde/PBS, DiI (Molecular Probes) crystals were needle injected into the cortex, allowed to diffuse for 4–8 weeks in 4% PFA at 37ºC, and then the brains were sectioned with a sliding microtome.

Histology and Immunohistochemistry

Brains were dissected and drop fixed for embryonic or neonatal brain, or perfusion fixed for adult with 4% paraformaldehyde/PBS. After cryoprotection in 30% sucrose/PBS, brain sections were obtained with a sliding microtome at 50 μm and stained according to standard protocols. Anti-DCLK N-terminal polyclonal antisera, 1:400; anti-DCLK C-terminal polyclonal antisera, 1:800; goat polyclonal anti-DCX (sc-8066, Santa Cruz Biotechnology), 1:400; rat monoclonal anti-L1CAM (Chemicon), 1:200; anti-testis-1 polyclonal antisera, 1:1000; anti-Tbr-1 polyclonal antisera, 1:100; anti-GFAP polyclonal antisera (DAKO), 1:1000; anti-calretinin polyclonal antisera (Swant), 1:200; and monoclonal anti-vimentin (Sigma), 1:200, were used per standard protocol.

BrdU Analysis

Pregnant mice were injected intraperitoneally with BrdU (sigma) at 100 μg/g body weight. Brains were fixed and treated with 2 N HCl, and BrdU-positive neurons were detected by immunostaining with monoclonal anti-BrdU (Becton Dickinson), 1:100, and Vector ABC detection system (Vector Laboratories).

RNAi Constructs

Oligonucleotides were ligated into the pGE2HRGFPII vector (Stratagene), which utilizes an EGFP reporter cassette on the same vector for identification of electroporated cells. The sequence of the two RNAi targets for DCLK was GGTTCGATTCTACAGAAAT and GGAATTGTGTATGCCATCT. For DCX, we used GGAGTGCGCTACATTTATA. The negative control scrambled sequence did not align with any known mammalian genes (Stratagene).

In Utero Electroporation

Pregnant CD1 dams were anesthetized with isoflurane, and the embryos visualized after laparotomy. Pulled capillary pipettes were filled with DNA solution (3–4 μg/μl) with 0.1% Fast Green for visualization of injection. Approximately 1 μl of DNA in injected into the lateral ventricle. A BTX Squarewave Electroporater ECM 830 was used to pass current across the brain at five pulses of 40 volts. This protocol resulted in embryonic lethality in approximately 25% of pups, but the remaining pups survived until euthanasia at E17.

Microscopy Imaging

Images were acquired with an inverted Nikon TE300 epifluorescent microscope, an Olympus FV1000 confocal microscope, or a DeltaVision image deconvolution microscope. Image processing was performed with MetaMorph or Softworks software.

Supplemental Data

The Supplemental Data for this article can be found online at http://www.neuron.org/cgi/content/full/49/1/55/DC1/.

Acknowledgments

We would like to acknowledge the University of California, San Diego Transgenic Core Facility for help with ES cell targeting and blastocyst injections, the University of California, San Diego Neurosciences Microscopy Core and Brendan Brinkman for imaging assistance, Robert McEvilly and Geoff Rosenfeld for Tst-1 antibody, Robert Hevner for Tbr-1 antibody, the O 'Leary and the LoTurco laboratory for help with siRNA technique and for the siRNA for DCX, the Ghosh laboratory for help with DiI injections, Anthony Wynshaw-Boris and Christopher Walsh for communicating unpublished results and for the Dcx knockout, Arthur Edelman for the DCLK-Cterm

and DCK2 antibodies, Jamie Marth for the pflox targeting vector, and Mario Capecchi for the TK1-TK2A vector. This work was supported by grants from the Epilepsy Foundation through the generous support of the American Epilepsy Society (T.T.) and the Milken Family Foundation (H.K.). Additional support was provided from the Searle Community Trust, the Merck Award in Developmental Disabilities, the Edwards Foundation, and the National Institutes of Health (NS41537, 42749, 47101, J.G.G.)

Received: May 31, 2005
Revised: August 29, 2005
Accepted: October 27, 2005
Published: January 4, 2006

References

Auladell, C., Perez-Sust, P., Super, H., and Soriano, E. (2000). The early development of thalamocortical and corticothalamic projections in the mouse. Anat. Embryol. (Berl.) *201*, 169–179.

Bai, J., Ramos, R.L., Ackman, J.B., Thomas, A.M., Lee, R.V., and LoTurco, J.J. (2003). RNAi reveals doublecortin is required for radial migration in rat neocortex. Nat. Neurosci. *6*, 1277–1283.

Burgess, H.A., and Reiner, O. (2000). Doublecortin-like kinase is associated with microtubules in neuronal growth cones. Mol. Cell. Neurosci. *16*, 529–541.

Burgess, H.A., and Reiner, O. (2002). Alternative splice variants of doublecortin-like kinase are differentially expressed and have different kinase activities. J. Biol. Chem. *277*, 17696–17705.

Caspi, M., Atlas, R., Kantor, A., Sapir, T., and Reiner, O. (2000). Interaction between LIS1 and doublecortin, two lissencephaly gene products. Hum. Mol. Genet. *9*, 2205–2213.

Caviness, V.S., Jr. (1982). Neocortical histogenesis in normal and reeler mice: a developmental study based upon [3H]thymidine autoradiography. Brain Res. *256*, 293–302.

Chang, L., Jones, Y., Ellisman, M.H., Goldstein, L.S., and Karin, M. (2003). JNK1 is required for maintenance of neuronal microtubules and controls phosphorylation of microtubule-associated proteins. Dev. Cell *4*, 521–533.

Chung, W.W., Lagenaur, C.F., Yan, Y.M., and Lund, J.S. (1991). Developmental expression of neural cell adhesion molecules in the mouse neocortex and olfactory bulb. J. Comp. Neurol. *314*, 290–305.

Corbo, J.C., Deuel, T.A., Long, J.M., LaPorte, P., Tsai, E., Wynshaw-Boris, A., and Walsh, C.A. (2002). Doublecortin is required in mice for lamination of the hippocampus but not the neocortex. J. Neurosci. *22*, 7548–7557.

Dawson, H.N., Ferreira, A., Eyster, M.V., Ghoshal, N., Binder, L.I., and Vitek, M.P. (2001). Inhibition of neuronal maturation in primary hippocampal neurons from tau deficient mice. J. Cell Sci. *114*, 1179–1187.

Del Rio, J.A., Gonzalez-Billault, C., Urena, J.M., Jimenez, E.M., Barallobre, M.J., Pascual, M., Pujadas, L., Simo, S., La Torre, A., Wandosell, F., et al. (2004). MAP1B is required for Netrin 1 signaling in neuronal migration and axonal guidance. Curr. Biol. *14*, 840–850.

des Portes, V., Pinard, J.M., Billuart, P., Vinet, M.C., Koulakoff, A., Carrie, A., Gelot, A., Dupuis, E., Motte, J., Berwald-Netter, Y., et al. (1998). A novel CNS gene required for neuronal migration and involved in X-linked subcortical laminar heterotopia and lissencephaly syndrome. Cell *92*, 51–61.

Dobyns, W.B., Truwit, C.L., Ross, M.E., Matsumoto, N., Pilz, D.T., Ledbetter, D.H., Gleeson, J.G., Walsh, C.A., and Barkovich, A.J. (1999). Differences in the gyral pattern distinguish chromosome 17-linked and X-linked lissencephaly. Neurology *53*, 270–277.

Edelman, A.M., Kim, W.Y., Higgins, D., Goldstein, E.G., Oberdoerster, M., and Sigurdson, W. (2004). Doublecortin kinase-2: a novel doublecortin-related protein kinase associated with terminal segments of axons and dendrites. J. Biol. Chem. *280*, 8531–8543.

Frantz, G.D., Bohner, A.P., Akers, R.M., and McConnell, S.K. (1994). Regulation of the POU domain gene SCIP during cerebral cortical development. J. Neurosci. *14*, 472–485.

Friocourt, G., Koulakoff, A., Chafey, P., Boucher, D., Fauchereau, F., Chelly, J., and Francis, F. (2003). Doublecortin functions at the extremities of growing neuronal processes. Cereb. Cortex *13*, 620–626.

Gambello, M.J., Darling, D.L., Yingling, J., Tanaka, T., Gleeson, J.G., and Wynshaw-Boris, A. (2003). Multiple dose-dependent effects of Lis1 on cerebral cortical development. J. Neurosci. *23*, 1719–1729.

Gleeson, J.G., Allen, K.M., Fox, J.W., Lamperti, E.D., Berkovic, S., Scheffer, I., Cooper, E.C., Dobyns, W.B., Minnerath, S.R., Ross, M.E., and Walsh, C.A. (1998). *doublecortin,* a brain-specific gene mutated in human X-linked lissencephaly and double cortex syndrome, encodes a putative signaling protein. Cell *92*, 63–72.

Gonchar, Y., and Burkhalter, A. (1997). Three distinct families of GABAergic neurons in rat visual cortex. Cereb. Cortex *7*, 347–358.

Gotz, M. (2003). Doublecortin finds its place. Nat. Neurosci. *6*, 1245–1247.

Gregory, W.A., Edmondson, J.C., Hatten, M.E., and Mason, C.A. (1988). Cytology and neuron-glial apposition of migrating cerebellar granule cells in vitro. J. Neurosci. *8*, 1728–1738.

Harada, A., Oguchi, K., Okabe, S., Kuno, J., Terada, S., Ohshima, T., Sato-Yoshitake, R., Takei, Y., Noda, T., and Hirokawa, N. (1994). Altered microtubule organization in small-calibre axons of mice lacking tau protein. Nature *369*, 488–491.

Hatten, M.E. (2002). New directions in neuronal migration. Science *297*, 1660–1663.

Hedin-Pereira, C., Lent, R., and Jhaveri, S. (1999). Morphogenesis of callosal arbors in the parietal cortex of hamsters. Cereb. Cortex *9*, 50–64.

Hevner, R.F., Shi, L., Justice, N., Hsueh, Y., Sheng, M., Smiga, S., Bulfone, A., Goffinet, A.M., Campagnoni, A.T., and Rubenstein, J.L. (2001). Tbr1 regulates differentiation of the preplate and layer 6. Neuron *29*, 353–366.

Hirotsune, S., Fleck, M.W., Gambello, M.J., Bix, G.J., Chen, A., Clark, G.D., Ledbetter, D.H., McBain, C.J., and Wynshaw-Boris, A. (1998). Graded reduction of Pafah1b1 (Lis1) activity results in neuronal migration defects and early embryonic lethality. Nat. Genet. *19*, 333–339.

Homma, N., Takei, Y., Tanaka, Y., Nakata, T., Terada, S., Kikkawa, M., Noda, Y., and Hirokawa, N. (2003). Kinesin superfamily protein 2A (KIF2A) functions in suppression of collateral branch extension. Cell *114*, 229–239.

Kato, M., and Dobyns, W.B. (2003). Lissencephaly and the molecular basis of neuronal migration. Hum. Mol. Genet. *12 Spec No 1*, R89–R96.

Kawaguchi, Y., and Kubota, Y. (1997). GABAergic cell subtypes and their synaptic connections in rat frontal cortex. Cereb. Cortex *7*, 476–486.

Kim, M.H., Cierpicki, T., Derewenda, U., Krowarsch, D., Feng, Y., Devedjiev, Y., Dauter, Z., Walsh, C.A., Otlewski, J., Bushweller, J.H., and Derewenda, Z.S. (2003). The DCX-domain tandems of doublecortin and doublecortin-like kinase. Nat. Struct. Biol. *10*, 324–333.

Laksok, M., Pichel, J.G., Gorman, J.R., Sauer, B., Okamoto, Y., Lee, E., Alt, F.W., and Westphal, H. (1996). Efficient in vivo manipulation of mouse genomic sequences at the zygote stage. Proc. Natl. Acad. Sci. USA *93*, 5860–5865.

Lavdas, A.A., Grigoriou, M., Pachnis, V., and Parnavelas, J.G. (1999). The medial ganglionic eminence gives rise to a population of early neurons in the developing cerebral cortex. J. Neurosci. *19*, 7881–7888.

Li, D.Y., Brooke, B., Davis, E.C., Mecham, R.P., Sorensen, L.K., Boak, B.B., Eichwald, E., and Keating, M.T. (1998). Elastin is an essential determinant of arterial morphogenesis. Nature *393*, 276–280.

Lin, P.T., Gleeson, J.G., Corbo, J.C., Flanagan, L., and Walsh, C.A. (2000). DCAMKL1 encodes a protein kinase with homology to doublecortin that regulates microtubule polymerization. J. Neurosci. *20*, 9152–9161.

Matsumoto, N., Pilz, D.T., and Ledbetter, D.H. (1999). Genomic structure, chromosomal mapping, and expression pattern of human DCAMKL1 (KIAA0369), a homologue of DCX (XLIS). Genomics *56*, 179–183.

Nedivi, E., Hevroni, D., Naot, D., Israeli, D., and Citri, Y. (1993). Numerous candidate plasticity-related genes revealed by differential cDNA cloning. Nature *363*, 718–722.

Noctor, S.C., Martinez-Cerdeno, V., Ivic, L., and Kriegstein, A.R. (2004). Cortical neurons arise in symmetric and asymmetric division zones and migrate through specific phases. Nat. Neurosci. *7*, 136–144.

Norris, C.R., and Kalil, K. (1991). Guidance of callosal axons by radial glia in the developing cerebral cortex. J. Neurosci. *11*, 3481–3492.

Ohshima, T., Ward, J.M., Huh, C.G., Longenecker, G., Veeranna, Pant H.C., Brady, R.O., Martin, L.J., and Kulkarni, A.B. (1996). Targeted disruption of the cyclin-dependent kinase 5 gene results in abnormal corticogenesis, neuronal pathology and perinatal death. Proc. Natl. Acad. Sci. USA *93*, 11173–11178.

Omori, Y., Suzuki, M., Ozaki, K., Harada, Y., Nakamura, Y., Takahashi, E., and Fujiwara, T. (1998). Expression and chromosomal localization of KIAA0369, a putative kinase structurally related to Doublecortin. J. Hum. Genet. *43*, 169–177.

Ozaki, H.S., and Wahlsten, D. (1993). Cortical axon trajectories and growth cone morphologies in fetuses of acallosal mouse strains. J. Comp. Neurol. *336*, 595–604.

Rash, B.G., and Richards, L.J. (2001). A role for cingulate pioneering axons in the development of the corpus callosum. J. Comp. Neurol. *434*, 147–157.

Reiner, O., Carrozzo, R., Shen, Y., Wehnert, M., Faustinella, F., Dobyns, W.B., Caskey, C.T., and Ledbetter, D.H. (1993). Isolation of a Miller-Dieker lissencephaly gene containing G protein beta-subunit-like repeats. Nature *364*, 717–721.

Shu, T., and Richards, L.J. (2001). Cortical axon guidance by the glial wedge during the development of the corpus callosum. J. Neurosci. *21*, 2749–2758.

Shu, T., Sundaresan, V., McCarthy, M.M., and Richards, L.J. (2003). Slit2 guides both precrossing and postcrossing callosal axons at the midline in vivo. J. Neurosci. *23*, 8176–8184.

Takei, Y., Teng, J., Harada, A., and Hirokawa, N. (2000). Defects in axonal elongation and neuronal migration in mice with disrupted tau and map1b genes. J. Cell Biol. *150*, 989–1000.

Tanaka, T., Serneo, F.F., Higgins, C., Gambello, M.J., Wynshaw-Boris, A., and Gleeson, J.G. (2004). Lis1 and doublecortin function with dynein to mediate coupling of the nucleus to the centrosome in neuronal migration. J. Cell Biol. *165*, 709–721.

Teng, J., Takei, Y., Harada, A., Nakata, T., Chen, J., and Hirokawa, N. (2001). Synergistic effects of MAP2 and MAP1B knockout in neuronal migration, dendritic outgrowth, and microtubule organization. J. Cell Biol. *155*, 65–76.

Xu, Q., Cobos, I., De La Cruz, E., Rubenstein, J.L., and Anderson, S.A. (2004). Origins of cortical interneuron subtypes. J. Neurosci. *24*, 2612–2622.

Yorke, C.H., Jr., and Caviness, V.S., Jr. (1975). Interhemispheric neocortical connections of the corpus callosum in the normal mouse: a study based on anterograde and retrograde methods. J. Comp. Neurol. *164*, 233–245.

Zhou, X., Suh, J., Cerretti, D.P., Zhou, R., and DiCicco-Bloom, E. (2001). Ephrins stimulate neurite outgrowth during early cortical neurogenesis. J. Neurosci. Res. *66*, 1054–1063.